Structural basis for transcription inhibition by *E. coli* SspA

Fulin Wang[1,2,3,†]**, Jing Shi**[4,5,†]**, Dingwei He**[6,7,†]**, Bei Tong**[8]**, Chao Zhang**[1]**, Aijia Wen**[4,5]**, Yu Zhang**[6,*]**, Yu Feng**[4,5,*] **and Wei Lin**[1,2,3,*]

[1]Department of Microbiology and Immunology, School of Medicine & Holistic Integrative Medicine, Nanjing University of Chinese Medicine, Nanjing, China, [2]State Key Laboratory of Natural Medicines, China Pharmaceutical University, Nanjing, China, [3]Jiangsu Collaborative Innovation Center of Chinese Medicinal Resources Industrialization, Nanjing 210023, China, [4]Department of Biophysics, Zhejiang University School of Medicine, Hangzhou, China, [5]Department of Pathology of Sir Run Run Shaw Hospital, Zhejiang University School of Medicine, Hangzhou, China, [6]Key Laboratory of Synthetic Biology, CAS Center for Excellence in Molecular Plant Sciences, Chinese Academy of Sciences, Shanghai, China, [7]University of Chinese Academy of Sciences, Beijing 100049, China and [8]Institute of Botany, Jiangsu Province and Chinese Academy of Sciences, Nanjing, China

ABSTRACT

Stringent starvation protein A (SspA) is an RNA polymerase (RNAP)-associated protein involved in nucleotide metabolism, acid tolerance and virulence of bacteria. Despite extensive biochemical and genetic analyses, the precise regulatory role of SspA in transcription is still unknown, in part, because of a lack of structural information for bacterial RNAP in complex with SspA. Here, we report a 3.68 Å cryo-EM structure of an *Escherichia coli* RNAP-promoter open complex (RPo) with SspA. Unexpectedly, the structure reveals that SspA binds to the *E. coli* σ^{70}-RNAP holoenzyme as a homodimer, interacting with σ^{70} region 4 and the zinc binding domain of *Eco*RNAP β' subunit simultaneously. Results from fluorescent polarization assays indicate the specific interactions between SspA and σ^{70} region 4 confer its σ selectivity, thereby avoiding its interactions with σ^s or other alternative σ factors. In addition, results from *in vitro* transcription assays verify that SspA inhibits transcription probably through suppressing promoter escape. Together, the results here provide a foundation for understanding the unique physiological function of SspA in transcription regulation in bacteria.

INTRODUCTION

Bacterial transcription initiation is carried out by a bacterial RNA polymerase (RNAP) holoenzyme comprising the bacterial RNAP core enzyme (subunit composition $\alpha_2\beta\beta'\omega$) and a σ factor (1). The primary σ factor (group-1 σ factor; σ^{70} in *Escherichia coli*; σ^A in Gram-positive bacteria) mediates transcription initiation at most housekeeping genes required for growth under normal conditions, while alternative σ factors, such as σ^s, direct the transcription of stress genes in response to metabolic, developmental and environmental signals. In addition, various transcription regulatory proteins also associate with RNAP in a dynamic manner to modulate the activity of RNAP in the process of transcription initiation, transcription elongation, and transcription termination (1).

The *E. coli* protein SspA was identified as a bacterial RNA polymerase-associated protein about 40 years ago and its expression was induced by glucose, nitrogen, phosphate or amino acid starvation (2,3). The reported physiological functions of *E. coli* SspA include responding to changes in the NTP pool of the cell through regulating the NTP kinase activities (4) and establishing the stationary phase-induced acid tolerance by downregulating the cellular level of H-NS (5–7). SspA is highly conserved among Gram-negative bacteria. Its orthologues in *Neisseria gonorrhoeae*, *Francisella novicida*, *Francisella tularensis* and *Vibrio cholerae* were shown to affect the expression of genes involved in pathogenesis (8–15). Intriguingly, SspA-like proteins are also present in higher organisms. Significant homologies between SspA and several stress- or auxin-regulated plant proteins have been also reported, suggesting that SspA may be a member of a highly conserved group of stress-induced proteins (3).

The crystal structure of SspA from *Haemophilus influenza*, *Pseudomonas fluorescens*, *Pseudomonas putida* and *Yersinia pestis* have been determined so far (16). SspA belongs to the cytosolic glutathione transferase (GST) family based on its structural similarity to canonical GST proteins, which are usually composed of two domains–a thioredoxin-like N-terminal domain and a larger C-terminal domain. The N-terminal domain constitutes the majority of GSH binding site, while the C-terminal domain contains the binding pocket for hydrophobic co-substrates (16). Although SspA is structurally similar to canonical GST proteins, it lacks the glutathione transferase activity and is different in the oligomerization. Instead, SspA regulates transcription in various bacteria by directly contacting RNAP through a conserved 'PHP' motif (17). Although many functional, biochemical, and structural studies of SspA have been performed in recent four decades, the molecular mechanism and structural basis of SspA-mediated transcription regulation is still unknown, partially because of a lack of precise structural information for bacterial RNAP in complex with SspA (3,4,6–10,12,17–20).

In this report, to gain insight into the functional role of SspA in transcription, we determined a single-particle cryo-electron microscopy (cryo-EM) structure of a *E. coli* RNAP-promoter open complex (RPo) with SspA at 3.68 Å resolution. The structure reveals that SspA bridges RNAP core enzyme and σ^{70} by making interactions both with zinc binding domain (ZBD) of RNAP-β' subunit and with a non-conserved patch on region 4 of the primary σ^{70} factor (σ^{70}R4). Further biochemical results confirmed the interactions between SspA and *E. coli* σ^{70}-RNAP and show that SspA inhibits transcription activity of *E. coli* σ^{70}-RNAP. Our structure with the biochemical results suggest SspA as a global transcription repressor of σ^{70} and such inhibition is probably through suppressing promoter escape. The results here provide the structural basis of SspA–RNAP interaction and a foundation for understanding the unique physiological function of SspA in transcription regulation of bacteria.

MATERIALS AND METHODS

SspA protein

Gene encoding *E. coli* *sspA* was synthesized and subcloned to pET28a by Sangon Biotech, Inc. *E. coli* strain BL21(DE3) (Invitrogen, Inc.) was transformed with plasmid pET28a-NH-SspA (Sangon Biotech, Inc) encoding N hexahistidine-tagged SspA under the control of the bacteriophage T7 promoter. Single colonies of the resulting transformants were used to inoculate 1 l LB broth containing 50 μg/ml kanamycin, cultures were incubated at 37°C with shaking until $OD_{600} = 0.6$, cultures were induced by addition of isopropyl-β-D-thiogalactoside (IPTG) to 0.5 mM, and cultures were incubated at 20°C overnight. Then, cells were harvested by centrifugation (5000 rpm; 10 min at 4°C), resuspended in 20 ml buffer A (20 mM Tris–HCl, pH 8.0, 0.1 M NaCl, 5% glycerol) and lysed using a ATS AH-10013 cell disrupter (ATS, Inc.). The lysate was centrifuged (12 000 rpm; 45 min at 4°C), and the supernatant was loaded onto a 2 ml column of Ni-NTA agarose (Qiagen,

Inc.) equilibrated with buffer A. The column was washed with 10 ml buffer A containing 0.16 M imidazole and eluted with 10 ml buffer A containing 0.5 M imidazole. The sample was further purified by anion-exchange chromatography on a Mono Q 10/100 GL column (GE Healthcare, Inc.; 160 ml linear gradient of 0.1–1.0 M NaCl in buffer A). Fractions containing SspA were pooled and stored at −80°C. SspA derivatives were expressed and purified in the same way as wild-type protein. The protein concentration is determined by using a BCA protein assay kit (Pierce™ BCA Protein Assay Kit, Thermo Scientific™, Inc.). Yields were ∼2 mg/l, and purities were >95%.

Alanine-substituted SspA derivatives were prepared as described for preparation of SspA, but using plasmid pET28a-SspA derivatives constructed using site-directed mutagenesis (QuikChange Site-Directed Mutagenesis Kit; Agilent).

E. coli σ^{70} protein

Escherichia coli σ^{70} protein was prepared using plasmid pGEMD as reported (21). Yield was ∼50 mg/l, and purity was >95%.

E. coli RNAP core enzyme

Escherichia coli RNAP core enzyme was prepared from *E. coli* strain BL21(DE3) (Invitrogen, Inc.) transformed with plasmid pIA900, using culture, induction and purification procedures essentially as reported (21). Yield was ∼2.5 mg/l, and purity was >95%.

Assembly of *E. coli* SspA–RPo complex

DNA oligonucleotides (sequences in Figure 1A) (Sangon Biotech, Inc.) were dissolved in nuclease-free water to ∼1 mM and stored at −80°C. Template strand DNA and non-template strand DNA were annealed at a 1:1 ratio in 10 mM Tris–HCl, pH 7.9, 0.2 M NaCl and stored at −80°C. *E. coli* SspA-RPo was prepared in reaction mixtures containing (500 μl): 9 μM σ^{70}, 18 μM SspA, 4.5 μM *E. coli* RNAP core enzyme and 5 μM DNA scaffold. *E. coli* σ^{70} protein was incubated with SspA for 10 min at 37°C, incubated with core for 10 min at 37°C and incubated with DNA scaffold for 10 min at 37°C. The mixture was applied to a Superose 6 Increase 10/300 GL column (GE Healthcare, Inc.) equilibrated in 10 mM HEPES, pH 7.5, 50 mM KCl, and the column was eluted with 24 ml of the same buffer. Fractions were checked by SDS-PAGE and the peak containing *E. coli* SspA-RPo complex was concentrated to 20 μM using an Amicon Ultra-0.5 ml centrifugal filter (10 kDa MWCO; Merck Millipore, Inc.).

Cryo-EM grid preparation

Immediately before freezing, 8 mM CHAPSO was added to the sample. C-flat grids (CF-1.2/1.3-4C; Protochips, Inc.) were glow-discharged for 60 s at 15 mA prior to the application of 3 μl of the complex, then plunge-frozen in liquid ethane using a Vitrobot (FEI, Inc.) with 95% chamber humidity at 10°C.

Figure 1. The overall structure of *E. coli* RNAP-promoter open complex with SspA. (**A**) The scaffold used in structure determination of *E. coli* RNAP-promoter open complex with SspA (SspA–RPo). (**B, C**) The orthogonal view orientations of the cryo-EM density map (**B**) and structure model (**C**) of *E. coli* transcription initiation complex with SspA. The RNAP, SspA and nucleic acids are presented as cartoon and colored as indicated in the color key. The density map is shown in gray envelop. The cryo-EM density map (blue transparent surface) for SspA. The cryo-EM density (red and yellow transparent surface) for the scaffold DNA and σ^{70}. NT, non-template-strand promoter DNA; T, template-strand promoter DNA.

Cryo-EM data acquisition and processing

The grids were imaged using a 300 kV Titan Krios (FEI, Inc.) equipped with a K2 Summit direct electron detector (Gatan, Inc.). Images were recorded with Serial EM in counting mode with a physical pixel size of 1.307 Å and a defocus range of 1.5–2.5 μm. Data were collected with a dose of 8 e/pixel/s. Images were recorded with a 12 s exposure and 0.25 s subframes to give a total dose of 59 e/Å². Subframes were aligned and summed using MotionCor2 (22). The contrast transfer function was estimated for each summed image using CTFFIND4 (23). From the summed images, ~10 000 particles were manually picked and subjected to 2D classification in RELION (24). 2D averages of the best classes were used as templates for auto-picking in RELION. Auto-picked particles were manually inspected, then subjected to 2D classification in RELION. Poorly populated classes were removed, resulting in a dataset of 610 066 particles. These particles were 3D classified in RELION using a map of *E. coli* RNAP-promoter open complex low-pass filtered to 40 Å resolution as a reference (25). 3D clas-

sification resulted in four classes. Particles in Class 1 (RPo) were 3D auto-refined and post-processed in RELION. Particles in Class 3 were subjected to an additional 3D classification and the class with density for SspA was 3D auto-refined and post-processed.

Cryo-EM model building and refinement

The models of RNAP core enzyme, σ^{70} and DNA scaffold from the structure of *E. coli* RPo (PDB 6CA0) (25), the crystal structure of SspA (PDB 1YY7) were fitted into the cryo-EM density map using Chimera (17,26). The model of nucleic acids was built manually in Coot (27). The coordinates were real-space refined with secondary structure restraints in Phenix (28).

Fluorescence polarization assay

The procedures of this fluorescence polarization assay were followed as previous reported with essential modifi-

Table 1. Single particle cryo-EM data collection, processing and model building for *Escherichia coli* RNAP-promoter open complex (RPo) with SspA

Data collection and processing	
Microscope	Titan Krios
Voltage (kV)	300
Detector	K2 summit
Electron exposure (e/Å^2)	59
Defocus range (μm)	1.5–2.5
Data collection mode	counting
Physical pixel size (Å/pixel)	1.307
Symmetry imposed	$C1$
Initial particle images	614,193
Final particle images	60,145
Map resolution (Å)^a	3.68
Refinement	
Map sharpening B-factor (Å)	−104
Root-mean-square deviation	
Bond length (Å)	0.007
Bond angle (°)	0.782
Molprobity statistics	2.93
Clashscore	11.70
Rotamer outliers (%)	10.60
Cβ outliers (%)	0.0
Ramachandran plot	99.88
Favored (%)	87.38
Outliers (%)	0.12

^{a}Gold-standard FSC 0.143 cutoff criteria.

cations (29–31). The reaction mixtures (100 μl) contain the fluorescein-labeled wild type SspA or SspA mutant derivatives (100 nM; final concentration) in FP buffer (PBS buffer) were incubated for 10 min at room temperature. *E. coli* σ^{70}-RNAP holoenzyme or *E. coli* σ^S-RNAP holoenzyme (a serial of final concentrations including 0, 3.5, 7, 14, 28, 56, 72, 96, 112, 120, 144, 168, 192, 216 and 240 μM) was added and incubated for 10 min at room temperature. The FP signals were measured using a plate reader (SPARK, TECAN, Inc.) equipped with an excitation filter of 485/20 nm and an emission filter of 520/20 nm. The data were plotted in SigmaPlot14.0 (Systat software, Inc) and the dissociation constant K_d was estimated by fitting the data to the following equation:

$$F = B[\text{S}] / (K_d + [\text{S}]) + F_0$$

where F is the FP signal at a given concentration of RNAP, F_0 is the FP signal in the absence of RNAP, [S] is the concentration of RNAP and B is an unconstrained constant, Error bars represent mean$\pm$ SEM out of $n = 3$ experiments.

In vitro multi-round transcription assays

Multi-round runoff transcription assays were carried out using *E. coli* σ^{70}-RNAPholoenzyme and wild-type *Eco*SspA or mutant derivatives through a mango method. For wild-type SspA concentration-dependent transcription activity measurements, the reaction (40 μl) was performed at 37°C and contained 100 nM N25 promoter Mango DNA, 100 nM *E. coli* σ^{70}-RNAP holoenzyme in reaction buffer [50 mM Tris–HCl, pH 8.0, 10 mM MgCl$_2$, 0.5% (vol/vol) glycerol, 100 mM potassium chloride, 1 mM DTT, 0.1% Tween-20]. Reaction was pre-incubated at 37°C for 5 min, and then 10 μl *Eco*SspA (a series of final concentrations including 0, 1.6, 3.2, 6.4, 12.8, 25.6 and 51.2 μM)

was added before the addition of the NTP mix (0.1 mM; final concentration) and Tol-biotin (0.5 mM; final concentration) incubated for 30 min. The fluorescence signals were measured using a plate reader (SPARK, TECAN, Inc.) at an excitation wavelength of 510 nm and an emission wavelength of 550 nm. The data were plotted in SigmaPlot14.0 (Systat software, Inc.), Error bars represent mean$\pm$ SEM out of $n = 3$ experiments. For evaluating the relative transcription activities between wild-type SspA and its mutants, the procedures and reaction system were similar as wild-type SspA concentration-dependent transcription activity measurements shown above except that wild-type SspA and its mutants concentration (25.6 μM final concentration) were added into the reaction system.

Electrophoretic mobility shift assay (EMSA) of *E. coli* RNAP-promoter open complex(RPo) with SspA

Template strand DNA oligonucleotide (5′-TCCCCTGC ATCCGTGACAGCTCCCATTATAGC ACAATTTA ACACTTTTGTCAATCATTTTGTT-3′, Sangon Biotech, Inc.) and non-template strand DNA oligonucleotide (5′-AACAAAATGATTGACAAAAGTGTTAAATTGTG CTAT AATGGGAGCTGTCACGGATGCAGGGGA-3′, Sangon Biotech, Inc.) were annealed at a 1:1 ratio in 10 mM Tris–HCl, pH 7.9, 0.2 M NaCl and stored at −80°C. Electrophoretic mobility shift assays were performed in reaction mixtures containing (20 μl): 0.4 μM wild type SspA or SspA mutant derivatives, 0.1 μM *E. coli* σ^{70}-RNAPholoenzyme, 0.05 μM DNA scaffold, 0.1mg/ml heparin, 7 mM Tris–HCl (pH 7.9), 50 mM Tris–Ac (pH 7.9), 0.19 M KGlu, 5 mM MgAc$_2$, 0.4 mM EDTA,0.2 mM DTT, 0.125 mg/ml BSA, 50 mM potassium phosphate (pH 6.5), 0.14 M NaCl and 22% glycerol. Wild type SspA protein incubated with *E. coli* σ^{70}-RNAP holoenzyme for 10 min at 37°C, then incubated with DNA scaffold for 10 min at 37°C, and incubated with 0.1 mg/ml heparin for 1 min at 37°C. The reaction mixtures were applied to 5% polyacrylamide slab gels (29:1 acrylamide/bisacrylamide), electrophoresed in 90 mM Tris-borate, pH 8.0, and 0.2 mM EDTA, stained with 4S Red Plus Nucleic Acid Stain (Sangon Biotech, Inc.) according to the procedure of the manufacturer, and analyzed by ImageJ (https://imagej.nih.gov/ij/).

Data analysis

Data for fluorescence polarization assays and *in vitro* multi-rounds transcription assays are means of three technical replicates. Error bars represent mean$\pm$ SEM out of $n = 3$ experiments.

RESULTS

Overall structure of *E. coli* RNAP-promoter open complex (RPo) with SspA

The Cryo-EM structure of *E. coli* RNAP-promoter open complex with SspA (SspA-RPo) was determined using a recombinant *E. coli* RNAPholoenzyme, a recombinant *E. coli* SspA, and a synthetic nucleic-acid scaffold comprising a 34-bp upstream dsDNA, a 16-bp downstream dsDNA, and a
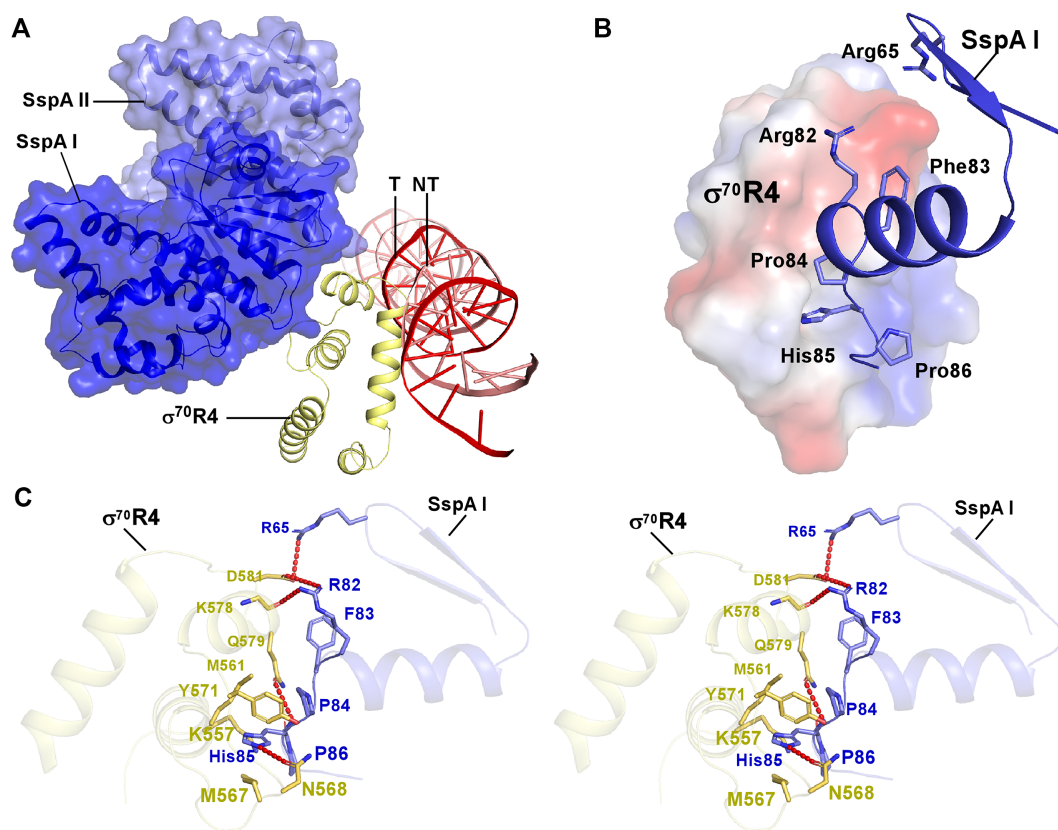
Figure 2. The interactions between SspA and the σ^{70}R4. (**A**) The relative location of SspA, σ^{70}R4 and upstream double strand DNA in the structure of *E. coli* RNAP-promoter open complex with SspA. (**B**) SspA interacted with negative surface of σ^{70}. The electrostatic potential surface of σ^{70} R4 was generated using APBS tools in Pymol. SspA is represented as a blue cartoon. (**C**) The detailed interactions between the σ^{70} R4 and SspA(stereo view). Hydrogen bonds are shown as red dashed lines.

noncomplementary transcription bubble with a consensus -10 element (Figure 1A) (21,32,33). The SDS-PAGE result confirmed that all protein components are present in the complex (Supplementary Figure S1B); and the EMSA result confirmed that the protein complex was able to bind the synthetic nucleic-acid scaffold DNA (Supplementary Figure S1C). The cryo-EM dataset was collected on Titan Krios and the particles were classified into 4 classes after 3D classification. The third Class, which shows clear presence of SspA and thereby represents SspA-RPo, was subjected 3D auto-refinement/post-process and finally refined to a 3.68 Å nominal resolution (Table 1; Figure 1B and C; Supplementary Figures S2–S5). The first class, which represents a regular RPo, was refined to a 3.58 Å nominal resolution (Table S1; Supplementary Figure S6 and S7). The cryo-EM map of SspA-RPo shows clear signals for *E. coli* σ^{70} RNAP holoenzyme, SspA and nucleic-acid scaffold (Supplementary Figure S5). The structures of *Eco*RNAP core enzyme and σ^{70} from SspA-RPo structure are very similar to the previously reported *E. coli* RNAP-promoter open complex (*E. coli* RPo) structure with a root-mean-square deviation (RMSD) of 1.33 Å (3694 Cαs aligned) (25). The region 2 of σ^{70} (σ^{70}R2) and the region 4 of σ^{70} (σ^{70}R4) interact with the conserved promoter –10 element and –35 element in a similar manner as they do in *E. coli* RPo. The crystal structure of *Yersinia pestis* SspA could be readily fit into the map, suggesting little conformational change of SspA upon inter-

action with *E. coli* σ^{70}-RNAPholoenzyme (Figure 1B and Supplementary Figure S2A).

The Cryo-EM structure of SspA–RPo clearly shows that *E. coli* SspA homodimer locates on the surface of the *E. coli* σ^{70}-RNAPholoenzyme (Figure 1B, C; Supplementary Figure S2). One SspA protomer (SspA I) mainly interacts with σ^{70}R4 through a large interface of ~483.5 Å^2 and the other SspA protomer (SspA II) contacts ZBD from RNAP-β' subunit through an interface of ~320.5 Å^2 (Figure 1B) (34). Both SspA I and SspA II approach the upstream edge of –35 element but make no direct contact with the promoter DNA (Figures 1B, C). Such interaction mode between SspA and σ^{70}-RPo supports the previous finding that SspA can bind to either RNAP core enzyme or RNAP holoenzyme using biochemical and genetic approaches (2,3,7,17). In addition, the Cryo-EM structure of SspA–RPo clearly reveals the interface of the SspA homodimer, which mainly involves the helices $\alpha 4-\alpha 5$ from both protomers and buries about 30% of the total surface area. The interface in our SspA-RPo structure is similar to that of *Y. pestis* SspA alone (Supplementary Figures S8A) (17), hinting that such homodimer interface is conserved and essential for physiological activities of SspA. Residues Arg73, Glu77, Tyr78, Glu81, Arg96 and Arg100 from $\alpha 4$ and $\alpha 5$ of both protomers form salt bridge and hydrogen bond networks stabilizing the interface. These hydrophilic residues are further surrounded by hydrophobic
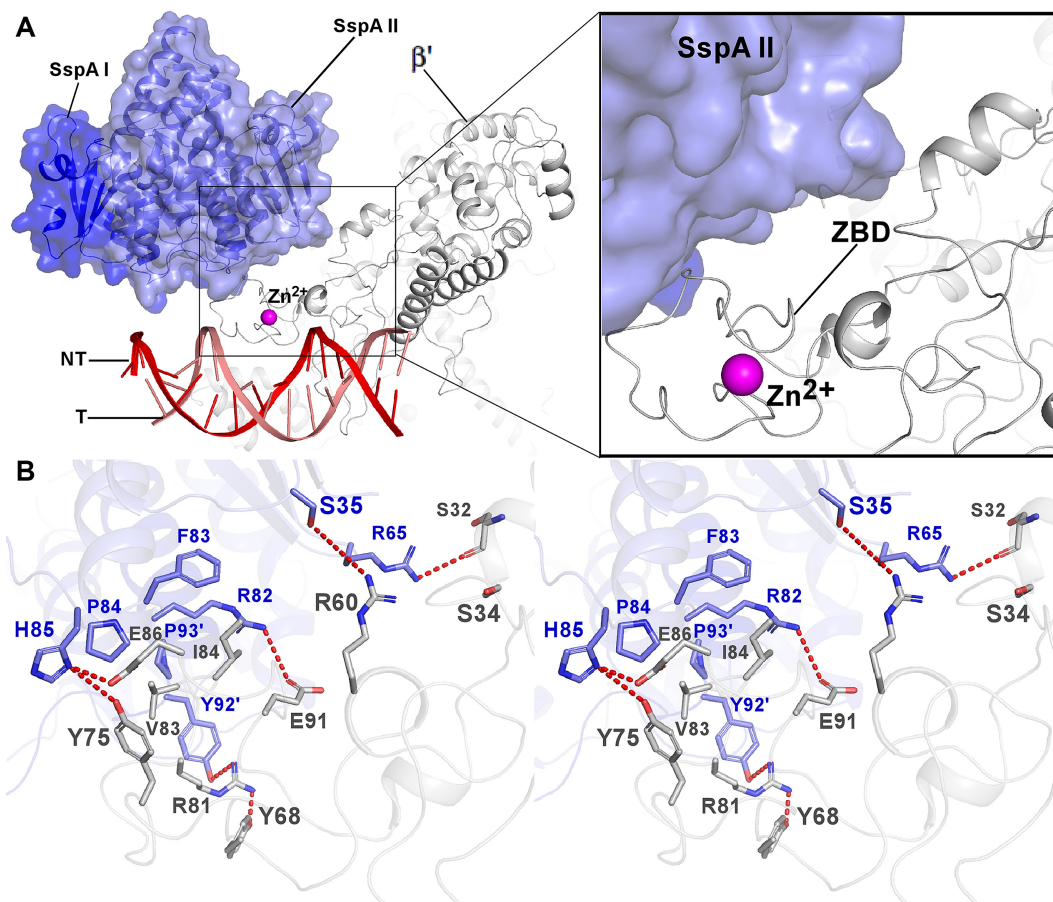
Figure 3. The interactions between SspA and the ZBD of RNAP-β′ subunit. (**A**) The relative location among SspA, σ70R4 and upstream double strand DNA. SspA II interacted with the zinc binding domain (ZBD) from RNAP-β′ subunit. SspA II is represented as a blue transparent surface and cartoon; ZBD from RNAP-β′ subunit is represented as cartoon. (**B**) The detailed interactions between the β′ subunit and SspA (stereo view). Salt-bridge bonds are shown as red dashed lines.

residues Leu69, Val94, Gly97 and Leu101, which protrude from α4 and α5 helices of SspA I and SspA II, strengthening the homodimer interactions (Supplementary Figures S8B). All of these structural observations are consistent with previous biochemical and genetic results (17), and match our fluorescence polarization assay result showing that G97I mutation disrupts the binding of *E. coli* SspA to RNAP holoenzyme (Supplementary Figures S8C) (12).

Interactions between SspA and σ70R4

In the cryo-EM structure of *E. coli* SspA-RPo, neither of SspA protomers contacts the non-template or template DNA, indicating that SspA may not affect the RNAP activities through interacting with the promoter directly as other typical transcription factors, such as CRP or NtrC of *E. coli* (35–38). The interactions between SspA I and σ70R4 include a polar interaction network, which consists of Arg65, Arg82, Pro84, His85 from SspA I and Asn568, Lys578, Gln579, Asp584 from σ70R4, and van del Waals interactions between residues of SspA I (Phe83, Pro84, His 85 and Pro86) and a hydrophobic shallow groove composed of several σ70R4 residues (Met561, Asn568, Lys557, Met567 and Tyr571 (Figure 2C). Specifically, residue His85, one of the highly conserved 'PHP' motif residues in SspA (17), is embedded into the shallow hydrophobic groove on σ70R4 (Fig-

ure 2A–C). Notably, most evolutionarily conserved residues of SspA, especially the 'PHP' motif, are clustered in the interface, implicating a functional relevance of its interaction with σ70 (Figure 2C). Moreover, the *E. coli* SspA derivative P84A/H85A/P86A loses the ability to support the acid resistance of *E. coli*, further suggesting the physiological importance of the SspA/σ70R4 interface (17).

Interactions between SspA and the ZBD of RNAP-β′ subunit

The structure also reveals specific interactions between SspA and the ZBD of RNAP-β′ subunit (Figure 3A). These interactions include, 1) direct polar interaction network made by Ser35, Arg65, Arg82 and His85 from SspA II and Ser32, Arg60, Glu86 and Glu91 from ZBD domain of RNAP-β′ subunit; 2) van der Waals interactions made by Phe83 and Pro84 from SspA II, Tyr 92 and Pro93 from SspA I, and Ser34, Arg81, Val83 and Ile84 from ZBD domain of RNAP-β′ subunit (Figure 3B).

We subsequently evaluated contribution of the interface residues to the SspA-σ70 and the SspA–ZBD interactions using fluorescence polarization assay. Previous studies suggested that a conserved 'PHP' motif within SspA is critical for the function of SspA and the binding of SspA to RNAP (17). In our structure, the 'PHP' motif plays an indispensable role in the interaction between SspA and σ70, consti-
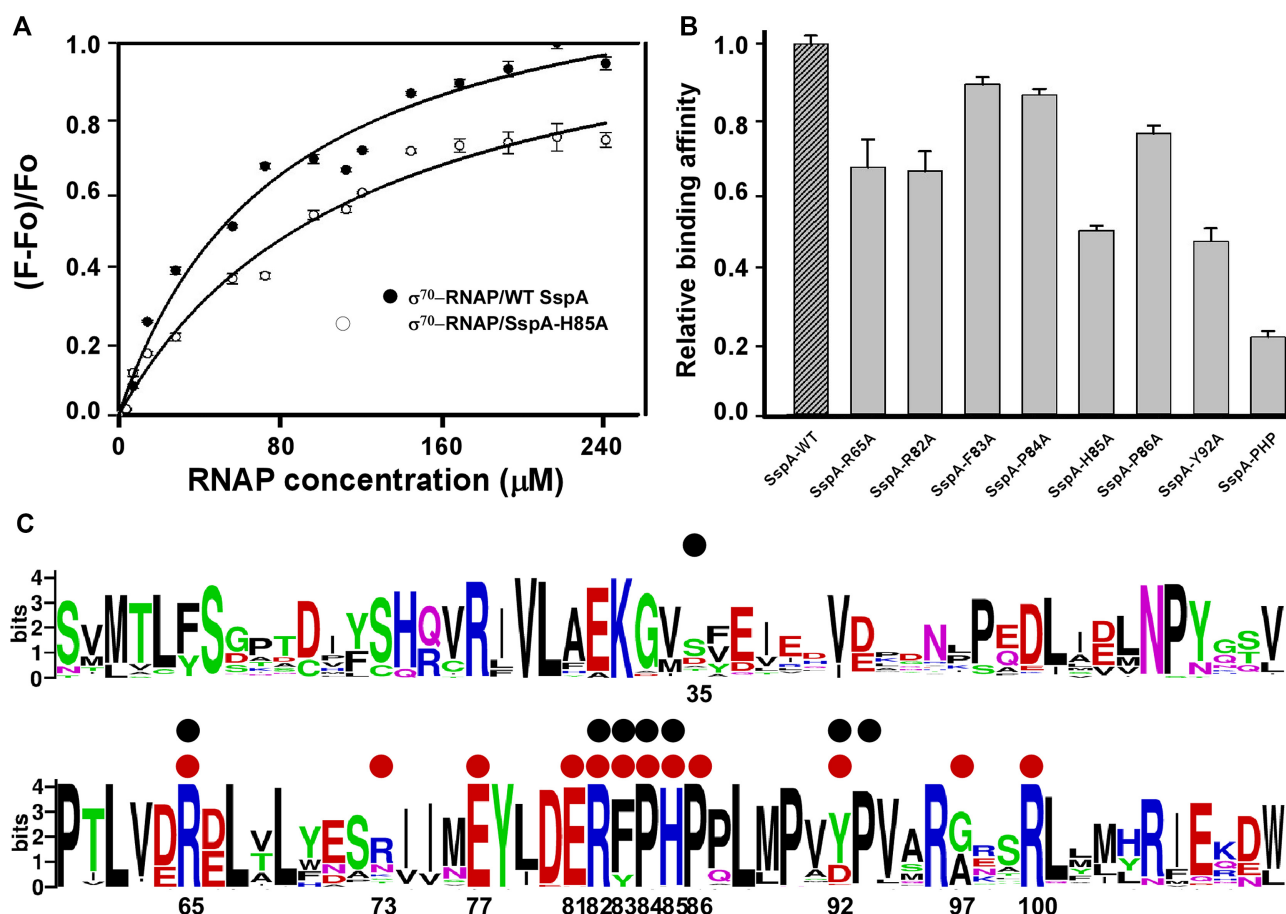
Figure 4. The interactions between SspA, the σ^{70}R4 and the ZBD of RNAP-β' subunit: binding affinity data. (**A**) Binding affinities between wild-type SspA or SspA-H85A and σ^{70}-RNAP measured by a fluorescence polarization (FP) assay. varying amounts of the σ^{70}-RNAP as indicated (mean ± SEM; three determinations). (**B**) Relative binding affinities of wild-type SspA and its mutants from the σ^{70}R4-SspA interface or ZBD of β' subunit-SspA interface measured by the fluorescence polarization assay (mean ± SEM; three determinations). Error bars represent mean± SEM out of $n = 3$ experiments. (**C**) Protein Sequence Alignments of SspA from ∼100 non-redundant bacterial species. The sequences were extracted from UniProt Database by BLAST. The alignment was performed by Cluster Omega and the sequence logos were generated on the WebLogo server (http://weblogo.berkeley.edu/logo.cgi). Black filled circles, residues involved in interactions with the ZBD from RNAP-β' subunit; Red filled circles indicate residues that are involved with interactions with σ^{70}R4. The residues are numbered as in *E. coli* SspA.

tuting part of the interface. Our results further show the triple mutation P84A/H85A/P86A of the 'PHP' motif, as well as single mutations (R65A, R82A, P84A, H85A or P86A), significantly impaired the SspA–RNAP interaction, validating our structure and highlighting the significance of the SspA-σ^{70} interface (Figure 4A, B). Our fluorescence polarization assay assessing effects of all possible alanine substitutions at the SspA-ZBD interface, including R65A, R82A, P84A, H85A and Y92A, also confirmed the significance of these residues observed in the cryo-EM structure (Figure 4B). Intriguingly, most evolutionarily conserved residues of SspA are clustered in the interfaces of SspA–ZBD and SspA-σ^{70}R4, implicating a functional relevance of the interaction of SspA with σ^{70} and RNAP-β' subunit (Figure 4C).

SspA inhibits transcription by stabilizing the association of σ^{70}R4 with RNAP core enzyme

A previous report showed that *Pseudomonas aeruginosa* SspA could function as an anti-σ^{70} factor involving in tran-

scription regulation of Alginate production (20). In our cryo-EM structure of SspA-RPo, *E. coli* SspA interacts with σ^{70}R4 and ZBD simultaneously (Figure 5A), suggesting SspA may act as a bridge and enhance the interactions between σ^{70}R4 and ZBD of RNAP-β' subunit. Considering that σ^{70}R4 serves as the hub for docking class II transcription activators but has to dissociate during promoter escape, we next explored the transcription output of the SspA–RNAP interaction.

To explore the effect of SspA on RNAP activities, we modified an fluorescence-based *in vitro* multi-round transcription assay (30,39). The results in Figure 5B show clear concentration-dependent transcription inhibition by the wild-type SspA, suggesting that SspA behaves as a transcription repressor. We subsequently evaluated the effect on transcription by alanine-substitution derivatives of SspA, which showed defect on binding to σ^{70}R4 or ZBD (Figures 4B). The results showed that most of the tested mutations (R65A, F83A, P84A, P86A, Y92A and P84A/H85A/P86A) reduced the transcription inhibition ability, suggesting that SspA-RNAP interaction accounts
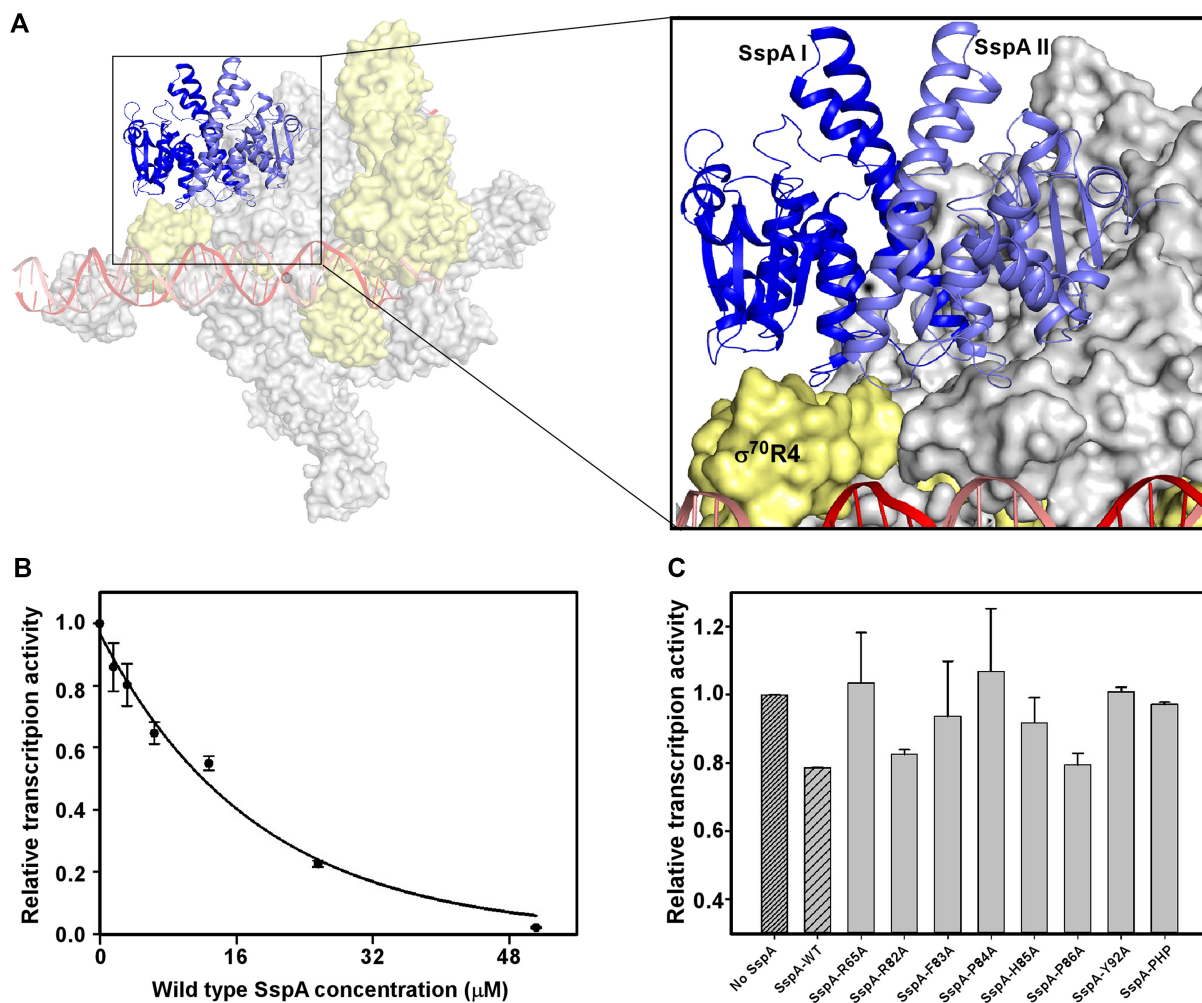
Figure 5. SspA inhibits promoter escape by interacting with the σ^{70}R4 and β' subunit of RNAP simultaneously. (**A**) Overall structure of *E. coli* σ^{70}-RNAP-promoter open complex shown in surface. SspA dimer was shown in cartoon. For clarity, α, β, β' and ω were represented as gray surface, other colors as in Figure 1. (**B**) Wild-type SspA concentration-dependent transcription activities evaluated by *in vitro* multi-rounds transcription assay. Each 40 μl reaction contains the *E. coli* σ^{70}-RNAP holoenzyme (100 nM), the fluorescence labelled mango N25 promoter DNA template (100 nM), and varying amounts of the wild-type SspA as indicated (mean $\pm$ SEM; three determinations). (**C**) Relative transcription activities of wild-type SspA and its mutants from the interface between SspA and ZBD of β' subunit to *E. coli* RNAP holoenzyme evaluated by the *in vitro* multi-rounds transcription assay (mean $\pm$ SEM; three determinations). Error bars represent mean$\pm$ SEM out of $n = 3$ experiments.

for the transcription inhibition of SspA (Figure 5C). The results lead to a hypothesis that SspA glues σ^{70}R4 and RNAP core enzyme, and inhibits promoter escape, a process requiring dissociation of both promoter and σ^{70}R4 from RNAP core enzyme (1,39–43)

SspA specifically inhibits transcription from σ^{70}-RNAP holoenzyme

Having demonstrated that SspA functions as a transcription repressor to inhibit σ^{70}-dependent gene transcription. We next asked whether SspA interacts with other alternative σ factors in *E. coli* and inhibits transcription initiated by these alternative σ factors. Sequence alignment of all six σ factors of *E. coli* reveals that the surface corresponding to SspA-interacting patch on σ^{70}R4 is not conserved among σ^{70} and other alternative σ factors; even for σ^S, the master stress σ factor that is most closely related σ^{70} in se-

quence and structure, there are six key interface residues (Lys557 versus Glu272, Met561 *vs.* Arg276, Met567 versus Gly282, Asn568 versus Tyr283, His571 versus Ala286, Asp581 versus Gly296; σ^{70} versus σ^S) different from those of σ^{70}R4 (Figure 6A–C). The sequence comparison suggests that SspA probably is a σ^{70}-specific transcription repressor. To validate such hypothesis, we tested the interaction between SspA and σ^S-RNAP holoenzyme. The results from fluorescence polarization assays clearly showed that SspA interacts with the σ^S-RNAP holoenzyme with a much lower affinity than that of σ^{70}-RNAP holoenzyme (Figure 6D), supporting SspA as a σ^{70}-specific transcription repressor. Furthermore, we also mutated the σ^{70} residue Lys557, Met567, Asn568, Tyr571, Gln579 and Asp581 to alanine in order to evaluate their effects on the binding affinities of SspA and σ^{70}-RNAP holoenzyme. The results clearly exhibited that these residues are critical for the SspA and σ^{70} interactions (Figure 6E), which is consistent with the con-
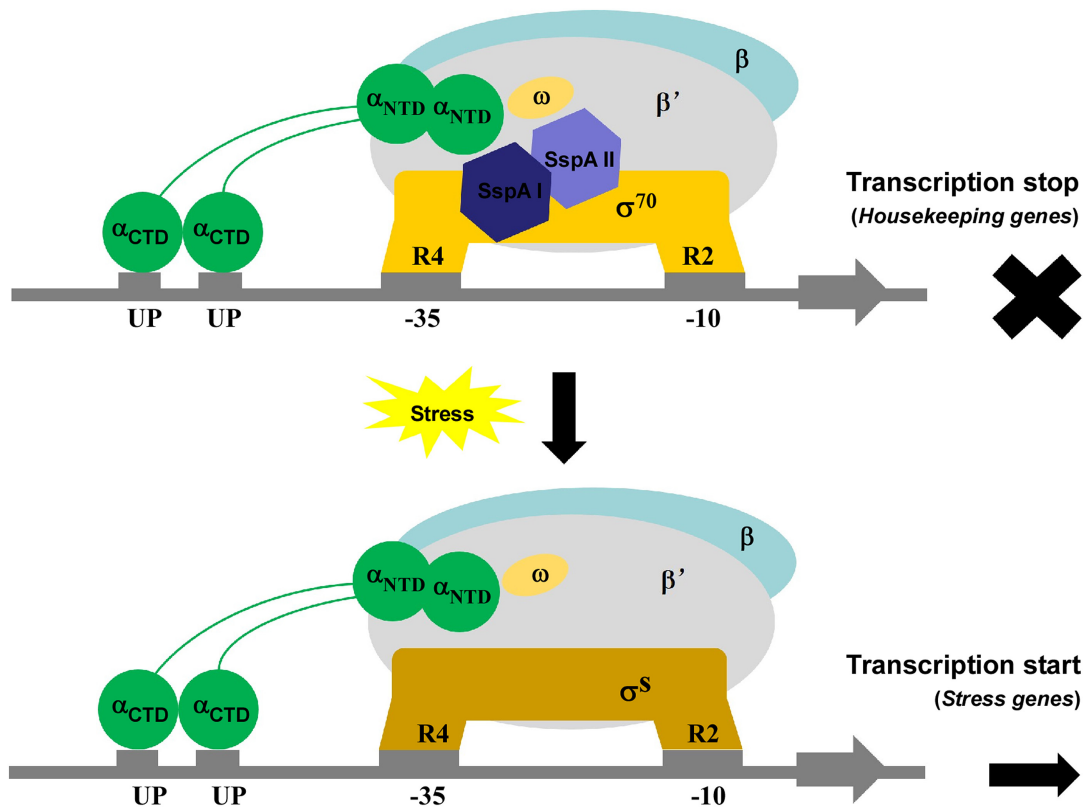
Figure 6. Protein–protein interactions between σ^{70} and σ^S and SspA. (**A**) Structure-based sequence alignment of potential SspA-interacting residues in *E. coli* σ^{70} and other alternative σ factors of *E. coli*. The non-conserved interaction residues are indicated with magenta stars; The secondary structure elements of σ^{70} is shown at the top. (**B**) Protein–protein interaction between σ^{70}R4 and SspA. (**C**) Protein–protein interaction between σ^SR4 and SspA. SspA, σ^{70}R4 and σ^SR4 are represented as cartoon colored in blue, yellow and wheat, respectively. (**D**) Binding affinities between σ^{70}-RNAP or σ^S-RNAP and wild-type SspA measured by a fluorescence polarization assay. varying amounts of the σ^{70}-RNAP or σ^S-RNAP as indicated (mean ± SEM; three determinations). (**E**) Relative binding affinities of wild-type σ^{70} and its region 4 mutants to *E.coli* RNAP core enzyme and wild-type SspA measured by the fluorescence polarization assay. Error bars represent mean± SEM out of $n = 3$ experiments.

Figure 7. Proposed working models of SspA. SspA inhibits the promoter escape process via interaction with σ^{70}R4 but not inhibit the promoter escape due to the absence of interaction with σ^{S}R4 under stress conditions.

clusion that SspA may act as a σ^{70}-specific transcription repressor.

DISCUSSION

SspA was discovered as an RNAP-associated protein ∼40 years ago. However, the physiological function of SspA in gene expression remains largely unclear. A large collection of biochemical, biophysical and genetic data imply that SspA may regulate transcription in an unprecedented manner (2,3,6–12,17–20). SspA is associated with the virulence of several pathogenic bacteria including *F. tularensis*, *N. gonorrhoeae*, *V. cholerae* and *enterohaemorrhagic E. coli* (EHEC) (6,8,9,15). *E. coli* SspA was shown to be required for acid resistance and transcriptional activation of phage P1 late genes. A recent report also suggested that *P. aeruginosa* SspA may function as an anti-σ^{70} factor (20). In this study, we show that SspA inhibits transcription activity of RNAP-σ^{70} holoenzyme and provide structural explanations for such inhibition.

Our cryo-EM structure of *E. coli* SspA-RPo shows that SspA acts as a stabilizing chaperon connecting σ^{70}_{4} and RNAP–β' ZBD of *E. coli* RNAP core enzyme but does not contact promoter DNA (Figure 1). The interface between SspA and RNAP-σ^{70} holoenzyme is relatively large (∼483.5 Å^2 in total) and comprises both hydrophobic and polar interactions. The interaction mode of RNAP-σ^{70} holoenzyme and SspA is in sharp contrast to the interaction mode of RNAP-σ^{70} holoenzyme and canonical class II transcription

activators, which typically make interaction with small activation patches on σ^{70}R4 through electrostatic interactions. We infer such difference of the interaction mode of canonical transcription activators and SspA to RNAP accounts for the difference of the consequences of their transcription regulation. The weak electrostatic interactions allow DNA-bound transcription activators to efficiently dock on RNAP-σ^{70} holoenzyme at the stage of RPo formation and to dissociate from the RNAP-σ^{70} holoenzyme at the stage of prompter escape without much obstacle. However, the large interface, made by both hydrophobic and hydrophilic interactions, between SspA and RNAP-σ^{70} holoenzyme tends to glue the σ^{70}R4 and RNAP core enzyme together, restricts the flexibility of σ^{70}R4 domain, which is believed to undergo substantial conformational change resulting in the dissociation of σ^{70}R4 during promoter escape process (1,39–43).

Most bacterial transcription factors repress gene expression by binding to DNA targets that overlap essential elements at their target promoters, thereby occluding access of RNAP (44). In many cases, repression is enhanced by the binding of multiple transcription repressor molecules at some promoters, which bind distally but interact with each other via DNA loops (44–46). At other promoters subjected to repression, RNAP is able to engage but is blocked at the promoter by the transcription repressor (44–46). A few transcription repressors, such as the CytR repressor, are anti-activators that simultaneously interact with their operator and adjacent activators, such as the cyclic AMP

(cAMP) receptor protein. At some promoters, CytR binding requires a combination of CytR–CRP and CytR–DNA interactions to prevent the binding of RNA polymerase (35,38). Therefore, it is widely accepted that transcription factors repress transcription mainly by sterically occluding the transcription machinery on promoter DNA (44,46).

However, there are also few examples of transcription repression requiring directly interaction between a repressor and RNA polymerase. For example, the P4 protein encoded by phage φ29, which infects *B. subtilis*, simultaneously binds to the C-terminal domain of the α-subunit of RNA polymerase and to the DNA upstream of the polymerase, thereby preventing promoter clearance (47). The SspA in principal fits into this category of transcription repressors, but differs in protein fold, RNAP-interacting mode, and probably the sub-steps of promoter escape that SspA acts on.

Collectively, we revealed here that SspA decreases the transcriptional activity of σ^{70}-RNAP in a DNA contact-independent manner and through stabilizing the key structural elements of σ^{70} and RNAP-β'subunit. Our study provides the structural basis and molecular mechanism of an unprecedented example of transcription repression. The transcription effect of SspA—repressing σ^{70}-dependent gene expression and facilitating σ^{s}-dependent stress-related gene expression—would help σ^{s}-RNAP to outcompete the transcription activity of housekeeping σ^{70}-RNAP and substantially increase the transcription activity of the σ^{s}-RNAP holoenzyme in the expression of stress-related genes (Figure 7). The unique DNA contact-independent mechanism also provides a new paradigm for bacterial transcription repression.

DATA AVAILABILITY

Atomic coordinates and structure factors for the cryo-EM structures of *E. coli* σ^{70} RNAP holoenzyme-SspA RNAP-promoter open complex has been deposited into the PDB and EMDB with accession codes PDB 7C97 and EMDB 30307, respectively. Atomic coordinates and structure factors for the cryo-EM structures of *E. coli* RNAP-promoter open complex has been deposited into the PDB and EMDB with accession codes PDB 7CHW and EMDB 30376, respectively.

SUPPLEMENTARY DATA

Supplementary Data are available at NAR Online.

ACKNOWLEDGEMENTS

REFERENCES

1. Feklistov,A., Sharon,B.D., Darst,S.A. and Gross,C.A. (2014) Bacterial sigma factors: a historical, structural, and genomic perspective. *Annu. Rev. Microbiol.*, **68**, 357–376.
2. Ishihama,A. and Saitoh,T. (1979) Subunits of RNA polymerase in function and structure. IX. Regulation of RNA polymerase activity by stringent starvation protein (SSP). *J. Mol. Biol.*, **129**, 517–530.
3. Williams,M.D., Ouyang,T.X. and Flickinger,M.C. (1994) Starvation-induced expression of SspA and SspB: the effects of a null mutation in sspA on *Escherichia coli* protein synthesis and survival during growth and prolonged starvation. *Mol. Microbiol.*, **11**, 1029–1043.
4. Shankar,S., Schlictman,D. and Chakrabarty,A.M. (1995) Regulation of nucleoside diphosphate kinase and an alternative kinase in *Escherichia coli*: role of the sspA and rnk genes in nucleoside triphosphate formation. *Mol. Microbiol.*, **17**, 935–943.
5. Bloch,V., Yang,Y., Margeat,E., Chavanieu,A., Auge,M.T., Robert,B., Arold,S., Rimsky,S. and Kochoyan,M. (2003) The H-NS dimerization domain defines a new fold contributing to DNA recognition. *Nat. Struct. Biol.*, **10**, 212–218.
6. Hansen,A.M. and Jin,D.J. (2012) SspA up-regulates gene expression of the LEE pathogenicity island by decreasing H-NS levels in enterohemorrhagic *Escherichia coli*. *BMC Microbiol.*, **12**, 231.
7. Hansen,A.M., Qiu,Y., Yeh,N., Blattner,F.R., Durfee,T. and Jin,D.J. (2005) SspA is required for acid resistance in stationary phase by downregulation of H-NS in *Escherichia coli*. *Mol. Microbiol.*, **56**, 719–734.
8. De Reuse,H. and Taha,M.K. (1997) RegF, an SspA homologue, regulates the expression of the *Neisseria gonorrhoeae* pilE gene. *Res. Microbiol.*, **148**, 289–303.
9. Charity,J.C., Blalock,L.T., Costante-Hamm,M.M., Kasper,D.L. and Dove,S.L. (2009) Small molecule control of virulence gene expression in *Francisella tularensis*. *PLoS Pathog.*, **5**, e1000641.
10. Charity,J.C., Costante-Hamm,M.M., Balon,E.L., Boyd,D.H., Rubin,E.J. and Dove,S.L. (2007) Twin RNA polymerase-associated proteins control virulence gene expression in *Francisella tularensis*. *PLoS Pathog.*, **3**, e84.
11. Cuthbert,B.J., Brennan,R.G. and Schumacher,M.A. (2015) Structural and biochemical characterization of the *Francisella tularensis* pathogenicity regulator, macrophage locus protein A (MglA). *PLoS One*, **10**, e0128225.
12. Cuthbert,B.J., Ross,W., Rohlfing,A.E., Dove,S.L., Gourse,R.L., Brennan,R.G. and Schumacher,M.A. (2017) Dissection of the molecular circuitry controlling virulence in *Francisella tularensis*. *Genes Dev.*, **31**, 1549–1560.
13. Grall,N., Livny,J., Waldor,M., Barel,M., Charbit,A. and Meibom,K.L. (2009) Pivotal role of the *Francisella tularensis* heat-shock sigma factor RpoH. *Microbiol*, **155**, 2560–2572.
14. Lauriano,C.M., Barker,J.R., Yoon,S.S., Nano,F.E., Arulanandam,B.P., Hassett,D.J. and Klose,K.E. (2004) MglA regulates transcription of virulence factors necessary for *Francisella*

tularensis intraamoebae and intramacrophage survival. *Proc. Natl. Acad. Sci. U.S.A.*, **101**, 4246–4249.

15. Merrell,D.S., Hava,D.L. and Camilli,A. (2002) Identification of novel factors involved in colonization and acid tolerance of *Vibrio cholerae*. *Mol. Microbiol.*, **43**, 1471–1491.

16. Sheehan,D., Meade,G., Foley,V.M. and Dowd,C.A. (2001) Structure, function and evolution of glutathione transferases: implications for classification of non-mammalian members of an ancient enzyme superfamily. *Biochem. J.*, **360**, 1–16.

17. Hansen,A.M., Gu,Y., Li,M., Andrykovitch,M., Waugh,D.S., Jin,D.J. and Ji,X. (2005) Structural basis for the function of stringent starvation protein a as a transcription factor. *J. Biol. Chem.*, **280**, 17380–17391.

18. Hansen,A.M., Lehnherr,H., Wang,X., Mobley,V. and Jin,D.J. (2003) *Escherichia coli* SspA is a transcription activator for bacteriophage P1 late genes. *Mol. Microbiol.*, **48**, 1621–1631.

19. Tsuzuki,M., Xu,X.Y., Sato,K., Abo,M., Arioka,M., Nakajima,H., Kitamoto,K. and Okubo,A. (2005) SspA, an outer membrane protein, is highly induced under salt-stressed conditions and is essential for growth under salt-stressed aerobic conditions in *Rhodobacter sphaeroides* f. sp. denitrificans. *Appl. Microbiol. Biotechnol.*, **68**, 242–250.

20. Yin,Y., Withers,T.R., Wang,X. and Yu,H.D. (2013) Evidence for sigma factor competition in the regulation of alginate production by *Pseudomonas aeruginosa*. *PLoS One*, **8**, e72329.

21. Feng,Y., Zhang,Y. and Ebright,R.H. (2016) Structural basis of transcription activation. *Science*, **352**, 1330–1333.

22. Zheng,S.Q., Palovcak,E., Armache,J.P., Verba,K.A., Cheng,Y. and Agard,D.A. (2017) MotionCor2: anisotropic correction of beam-induced motion for improved cryo-electron microscopy. *Nat. Methods*, **14**, 331–332.

23. Rohou,A. and Grigorieff,N. (2015) CTFFIND4: Fast and accurate defocus estimation from electron micrographs. *J. Struct. Biol.*, **192**, 216–221.

24. Scheres,S.H. (2012) RELION: implementation of a Bayesian approach to cryo-EM structure determination. *J. Struct. Biol.*, **180**, 519–530.

25. Narayanan,A., Vago,F.S., Li,K., Qayyum,M.Z., Yernool,D., Jiang,W. and Murakami,K.S. (2018) Cryo-EM structure of *Escherichia coli* sigma(70) RNA polymerase and promoter DNA complex revealed a role of sigma non-conserved region during the open complex formation. *J. Biol. Chem.*, **293**, 7367–7375.

26. Pettersen,E.F., Goddard,T.D., Huang,C.C., Couch,G.S., Greenblatt,D.M., Meng,E.C. and Ferrin,T.E. (2004) UCSF Chimera–a visualization system for exploratory research and analysis. *J. Comput. Chem.*, **25**, 1605–1612.

27. Emsley,P. and Cowtan,K. (2004) Coot: model-building tools for molecular graphics. *Acta Crystallogr. D Biol. Crystallogr.*, **60**, 2126–2132.

28. Adams,P.D., Afonine,P.V., Bunkoczi,G., Chen,V.B., Davis,I.W., Echols,N., Headd,J.J., Hung,L.W., Kapral,G.J., Grosse-Kunstleve,R.W. *et al.* (2010) PHENIX: a comprehensive Python-based system for macromolecular structure solution. *Acta Crystallogr. D Biol. Crystallogr.*, **66**, 213–221.

29. Hubin,E.A., Fay,A., Xu,C., Bean,J.M., Saecker,R.M., Glickman,M.S., Darst,S.A. and Campbell,E.A. (2017) Structure and function of the mycobacterial transcription initiation complex with the essential regulator RbpA. *ELife*, **6**, e22520.

30. Xu,J., Cui,K., Shen,L., Shi,J., Li,L., You,L., Fang,C., Zhao,G., Feng,Y., Yang,B. *et al.* (2019) Crl activates transcription by stabilizing active conformation of the master stress transcription initiation factor. *ELife*, **8**, e50928.

31. Lin,W., Mandal,S., Degen,D., Liu,Y., Ebright,Y.W., Li,S., Feng,Y., Zhang,Y., Mandal,S., Jiang,Y. *et al.* (2017) Structural basis of *Mycobacterium tuberculosis* transcription and transcription inhibition. *Mol. Cell*, **66**, 169–179.

32. Bae,B., Feklistov,A., Lass-Napiorkowska,A., Landick,R. and Darst,S.A. (2015) Structure of a bacterial RNA polymerase holoenzyme open promoter complex. *ELife*, **4**, e08504.

33. Zuo,Y. and Steitz,T.A. (2015) Crystal structures of the E. coli transcription initiation complexes with a complete bubble. *Mol. Cell*, **58**, 534–540.

34. Lane,W.J. and Darst,S.A. (2010) Molecular evolution of multisubunit RNA polymerases: sequence analysis. *J. Mol. Biol.*, **395**, 671–685.

35. Valentin-Hansen,P., Sogaard-Andersen,L. and Pedersen,H. (1996) A flexible partnership: the CytR anti-activator and the cAMP-CRP activator protein, comrades in transcription control. *Mol. Microbiol.*, **20**, 461–466.

36. Yang,X.F., Ji,Y., Schneider,B.L. and Reitzer,L. (2004) Phosphorylation-independent dimer-dimer interactions by the enhancer-binding activator NtrC of *Escherichia coli*: a third function for the C-terminal domain. *J. Biol. Chem.*, **279**, 36708–36714.

37. Lawson,C.L., Swigon,D., Murakami,K.S., Darst,S.A., Berman,H.M. and Ebright,R.H. (2004) Catabolite activator protein: DNA binding and transcription activation. *Curr. Opin. Struct. Biol.*, **14**, 10–20.

38. Busby,S. and Ebright,R.H. (1999) Transcription activation by catabolite activator protein (CAP). *J. Mol. Biol.*, **293**, 199–213.

39. Shi,J., Gao,X., Tian,T., Yu,Z., Gao,B., Wen,A., You,L., Chang,S., Zhang,X., Zhang,Y. *et al.* (2019) Structural basis of Q-dependent transcription antitermination. *Nat. Commun.*, **10**, 2925.

40. Yin,Z., Kaelber,J.T. and Ebright,R.H. (2019) Structural basis of Q-dependent antitermination. *Proc. Natl. Acad. Sci. USA*, **116**, 18384–18390.

41. Kulbachinskiy,A. and Mustaev,A. (2006) Region 3.2 of the sigma subunit contributes to the binding of the 3'-initiating nucleotide in the RNA polymerase active center and facilitates promoter clearance during initiation. *J. Biol. Chem.*, **281**, 18273–18276.

42. Pupov,D., Kuzin,I., Bass,I. and Kulbachinskiy,A. (2014) Distinct functions of the RNA polymerase sigma subunit region 3.2 in RNA priming and promoter escape. *Nucleic Acids Res.*, **42**, 4494–4504.

43. Li,L., Molodtsov,V., Lin,W., Ebright,R.H. and Zhang,Y. (2020) RNA extension drives a stepwise displacement of an initiation-factor structural module in initial transcription. *Proc. Natl. Acad. Sci. U.S.A.*, **117**, 5801–5809.

44. Browning,D.F. and Busby,S.J. (2016) Local and global regulation of transcription initiation in bacteria. *Nat. Rev. Microbiol.*, **14**, 638–650.

45. Balleza,E., López-Bojorquez,L.N., Martínez-Antonio,A., Resendis-Antonio,O., Lozada-Chávez,I., Balderas-Martínez,Y.I., Encarnación,S. and Collado-Vides,J. (2008) Regulation by transcription factors in bacteria: beyond description. *FEMS Microbiol. Rev.*, **33**, 133–151.

46. Browning,D.F., Butala,M. and Busby,S.J.W. (2019) Bacterial transcription factors: regulation by pick "N" mix. *J. Mol. Biol.*, **431**, 4067–4077.

47. Monsalve,M., Calles,B., Mencia,M., Rojo,F. and Salas,M. (1998) Binding of phage phi29 protein p4 to the early A2c promoter: recruitment of a repressor by the RNA polymerase. *J. Mol. Biol.*, **283**, 559–569.